GSI

GSI-91-31
PREPRINT
JUNI 1991

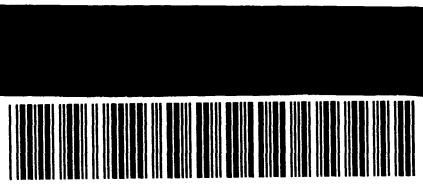

CM-P00063111

GAMOW-TELLER BETA DECAY OF THE VERY NEUTRON-DEFICIENT N=50 NUCLIDE ^{98}Cd

A PLOCHOCKI, K. RYKACZEWSKI, T. BATSCH, J. SZERYPO,
J. ZYLICZ, R. BARDEN, O. KLEPPER, E. ROECKL, D. SCHARDT,
H. GABELMANN, P. HILL, H. RAVN, T. THORSTEINSEN, I.S. GRANT,
H. GRAWE, P. MANAKOS, L.D. SKOURAS
AND THE ISOLDE COLLABORATION

Gesellschaft für Schwerionenforschung mbH
Planckstr. 1 · Postfach 11 05 52 · D-6100 Darmstadt 11 · Germany

Gamow-Teller Beta Decay of the Very Neutron-Deficient N=50 Nuclide ^{98}Cd *)

A. Plochocki, K. Rykaczewski, T. Batsch, J. Szerypo, J. Zylicz
Institute of Experimental Physics, Warsaw University, PL-00-681 Warsaw, Poland

R. Barden, O. Klepper, E. Roeckl, D. Schardt
GSI, D-6100 Darmstadt, Federal Republic of Germany

H. Gabelmann, P. Hill, H. Ravn, T. Thorsteinsen
CERN-ISOLDE, CH-1211 Geneva, Switzerland

I.S. Grant
Schuster Laboratories, University of Manchester, Manchester M13 9PL, UK

H. Grawe
HMI, D-1000 Berlin, Federal Republic of Germany

P. Manakos
Technische Hoschschule Darmstadt, D-6100 Darmstadt,
Federal Republic of Germany

L. D. Skouras
Institue of Nuclear Physics, NCSR Demokritos,
GR-15310 Aghia Paraskevi, Greece

and the ISOLDE Collaboration

PACS: 23.40.Hc, 21.10.Dr, 21.10Pc

*) Dedicated to Prof. P. Armbruster on the occasion of his 60th birthday

Abstract

For the first time, detailed decay-spectroscopic investigations were performed for the very neutron-deficient N = 50 nuclide ^{98}Cd . The ^{98}Cd activity was produced in spallation reactions between 600 MeV protons and a natural tin target, yielding a ^{98}Cd beam intensity of 10 to 60 atoms per second at the collector of the ISOLDE mass-separator. By means of γ-ray and conversion-electron spectroscopy, 19 transitions were found to follow the β^+ /EC decay $^{98}Cd \rightarrow {}^{98}$Ag. The transitions at 61 and 107 keV were shown to be M1(+E2) and E2, respectively, and the ^{98}Cd half-life was measured as 9.2 ± 0.3 s. The Q_{EC} value of ^{98}Cd is determined semiempirically and is compared to model predictions together with the measured Q_{EC} values of the N = 50 isotones ^{92}Mo, ^{94}Ru, and ^{96}Pd taken from the literature. The newly established decay scheme of ^{98}Cd includes 9 excited states of ^{98}Ag. Four states at 1691, 1861, 2164, and 2544 keV are directly fed by $0^+ \rightarrow 1^+$ Gamow-Teller beta transitions with a summed strength of $3.5\ ^{+0.8}_{-0.7}$. This value corresponds to $25 \pm 5\%$ of the strength predicted for the GT transformation of a $g_{9/2}$ proton (in ^{98}Cd) into a $g_{7/2}$ neutron (in ^{98}Ag) by the extreme single-particle shell model with pairing. The GT-strength splitting and quenching, observed for ^{98}Cd, are compared with the corresponding data for lighter even-even N = 50 isotones, and are discussed with reference to the predictions of more sophisticated nuclear models. Within the framework to the shell-model, we find that it is possible to explain qualitatively the observed GT strength distribution and its total magnitude without renormalizing the free-neutron value of the axial-vector coupling constant.

1.Introduction

The EC/β^+ decay of ^{98}Cd is of particular interest for studying the quenching [1,2] and splitting [3] of the $g_{9/2} \rightarrow g_{7/2}$ Gamow-Teller (GT) decay strength: The even N = 50 isotones ^{94}Ru and ^{96}Pd have already been investigated [4,5] and ^{98}Cd is thus the last one of these isotones on the way to the presently undetectable doubly-closed-shell nuclide ^{100}Sn.

The neutron-deficient nuclide ^{98}Cd is far away from the line of beta stability. Until now it has been produced in amounts sufficient for spectroscopic investigations only at ISOLDE. Using this facility, first results on ^{98}Cd decay have been reported by Elmroth et al. [6]. Their measurements were performed with a plastic β-counter having nearly 4π geometry. In the decay of mass-separated sources at A = 98, a β-particle component was observed with a half-life of about 8 s, which was tentatively ascribed to ^{98}Cd. Some evidence for 61 and 107 keV transitions in ^{98}Ag, following the decay of ^{98}Cd, was obtained later in conversion-electron and γ/X-ray studies of A = 98 samples, performed in connection with the investigation of ^{100}Cd decay [7] . In this study, the half-life of ^{98}Cd was determined to be 8.1 ± 0.5 *s*.

In the experiment described here, which was entirely devoted to the study of ^{98}Cd, this activity was identified unambiguously, the preliminary assignment of the two above-mentioned transitions was confirmed, and additional γ-ray and conversion-electron data were obtained. A decay scheme is proposed for ^{98}Cd, and the semiempirically deduced Q_{EC} value as well as the observed GT strength are discussed, together with relevant data for neighbouring nuclei, in comparison with nuclear-model predictions.

2. Experimental Techniques

The neutron-deficient isotopes of cadmium were produced by spallation of a natural-tin target with 600 MeV protons. The ISOLDE facility provided mass-separated beams of these isotopes with little contamination from direct production of the isobaric silver nuclei [7,8]. Using these beams, mass-separated samples were collected on a tape and moved to counting stations after fixed time intervals. For ^{98}Cd this interval was 16 seconds.

The maximum production rates for ^{102}Cd, ^{100}Cd , and ^{98}Cd, normalized to a proton beam intensity of 1μA, were respectively 10^6 , $7x10^4$, and 40 atoms per second at the collector of the mass separator. This decrease of the yield with increasing distance from the line of stability is caused primarily by the decrease of the production cross section. For ^{98}Cd, additionally, the release efficiency from the target/ion-source sys-

tem is lower than for the heavier cadmium isotopes. This is due to the fact that even at the highest ion-source temperatures, the diffusion time of radioactive atoms out of the liquid-tin target is considerably longer than the half-life of ^{98}Cd.

The information on ^{98}Cd decay was obtained in two experiments. For the first one, the detection systems at the counting stations were (a) a mini-orange electron spectrometer [9] and a 20% γ/X Ge(i) detector; (b) an X-ray Ge(i) detector, with an energy resolution (FWHM) of 500 eV, and a 65% Ge(i) detector. In both arrangements the detectors were on opposite sides of the transport tape. During the first experiment, the production rate was 10 to 20 atoms per second at the collector. Because of this low activity level, a close geometry was used. The detection efficiency of the γ-ray detectors was about 10% for the peak of the γ-ray energy-dependent efficiency characteristic, which led to large summing effects. In the arrangement (b), the tape passed through a thin plastic scintillator covering nearly 4π geometry. Thus, the γ- and X-ray detectors could be gated with betas. This was necessary in order to be able to discriminate ^{98}Cd γ/X rays against the large background present in the ISOLDE experimental area.

In the second experiment, only γ-ray measurements were performed. Compared to the previous experiment, the quality of the γ- data was improved. This was due to the higher production rate of ^{98}Cd , which amounted to about 65 atoms per second, and to the use of an array of four Ge detectors. The standard efficiency of these detectors was 70, 30, 28, and 23%. In order to reduce summing effects, the first two of them were covered, respectively, with a 2 mm thick tin absorber and an absorber consisting of 2 mm thick lead, 2.5 mm thick brass and 5 mm thick aluminium dics. Moreover, the detectors were further away from the source position compared to the first experiment, their maximum efficiencies for photo-peak detection being now between 0.3 and 3%, and a 180^{o} geometry was avoided for all detector pairs. The reduction of summing compensated in part for the count-rate decrease resulting from the lower solid angles of the detectors. Some limitation of the results arose from a contribution of molecular-ion contaminants, especially $^{75}Br\,^{23}Na^{+}$. For unknown reasons, these contaminants were three orders-of-magnitude higher (relative to ^{98}Cd) than in the first experiment.

In both runs, coincidence events were collected on an event-by-event basis, while the single spectra for all detectors and the beta gated γ/X-ray spectra were collected in an 8 x 2 s multispectrum mode.

3. Experimental Results

3.1 Gamma and Conversion-Electron Measurements

A detailed analysis of all singles and coincidence spectra (see e.g. Figs. 1 and 2), led to the identification of 19 transitions that follow the $^{98}Cd \rightarrow {}^{98}Ag$ decay (see Table 1). For a few intense γ-transitions, the identification is based on the observation of coincidences with both the silver KX-rays and the annihilation radiation. The assignment of weaker transitions results from their coincidence with the intense ones. The five lines above 1600 keV could be seen only after summing the spectra that were gated by KX-rays and by the three lowest-energy transitions (see Fig. 2). A comparison of the γ-ray spectra from the first and second experiment allowed us to reject some lines that resulted entirely from summing of cascading transitions, and to estimate intensity corrections for real cross-over transitions. For this purpose, the absolute-efficiency curves were used as obtained with standard sources. From the multispectrum analysis of γ-ray intensities, the half-life of ^{98}Cd was found to be 9.2 ± 0.3 s.

Internal conversion lines were observed only for the 61 and 107 keV transitions (see Fig. 3). The energies determined for the K and (L + M) conversion lines represent independent evidence for assigning these transitions to ^{98}Ag. The K-conversion coefficients of the 61 and 107 keV transitions were determined by comparing the electron/gamma intensities with those measured under identical conditions for M1 transitions at 58.9, 97.4, 111.4, 116.0, 124.7, and 139.7 keV in ^{100,101,102}Ag [11]. As can be seen from Table 2, these coefficients indicate the M1(+E2) and E2 character of the 61 and 107 keV transitions, respectively. The observed K/(L+M) conversion-coefficient ratios are consistent with these multipolarity assignments.

3.2 The ^{98}Cd Decay Scheme

In Fig. 4, a decay scheme of ^{98}Cd is shown that contains nine levels of ^{98}Ag and accounts for all but one of the 19 transitions, listed in Table 1, as well as for the measured coincidence data. The decay energy Q_{EC} used to calculate the log ft values is discussed in Sect. 4.2.

The four ^{98}Ag levels with the highest observed excitation energies are directly fed by the EC/β^+ transitions with log ft $\leq$ 4.2. This indicates the spin and parity assignment 1^+. We neglect here feeding of these levels by undetected weak γ-transitions from still higher-lying levels. Such feeding would correspond to beta branching ratios that are lower than those shown in Fig. 4. For the strongly fed level

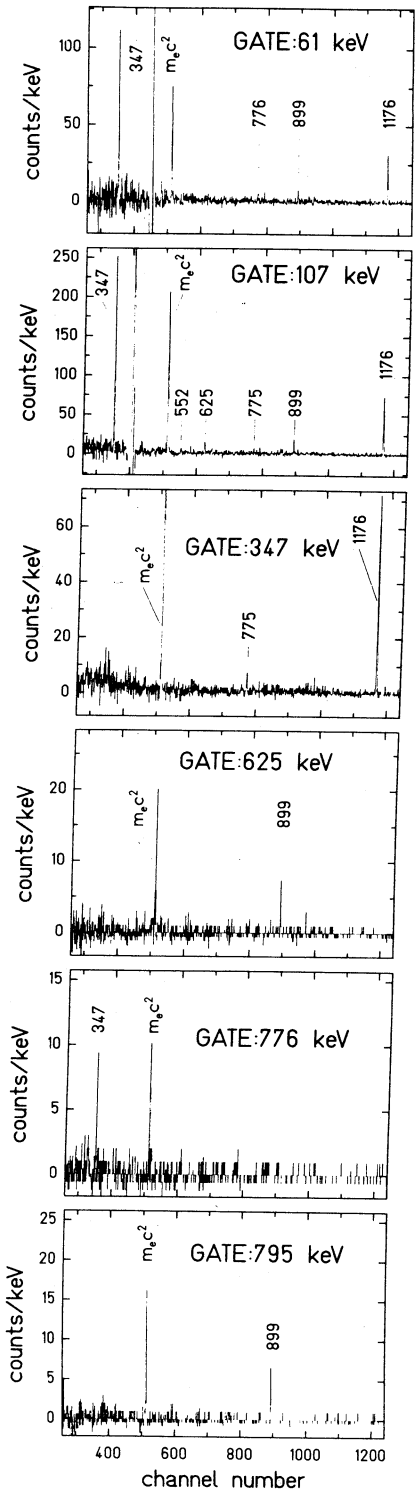

Fig. 1. Spectra of γ-rays from the decay of ^{98}Cd , recorded in the 70% Ge detector (26 h of data acquisition). The spectra were gated, respectively, by 61 keV, 107 keV, 347 keV, 625 keV, 776 keV, and 795 keV γ-lines measured with the 28% detector. In the spectra gated with 61 keV and 107 keV γ lines, the peak structures observed at 450 keV and 404 keV do not represent gamma.-transitions in ^{98}Ag. The occurrence of these structures , whose energies correspond to the differences between 511 keV and the energy of the gate transition, is due to scattering of annihilation quanta between the detectors. Accordingly, the backround-subtraction windows on either side of the gate γ-ray cause the dips next to these peaks.

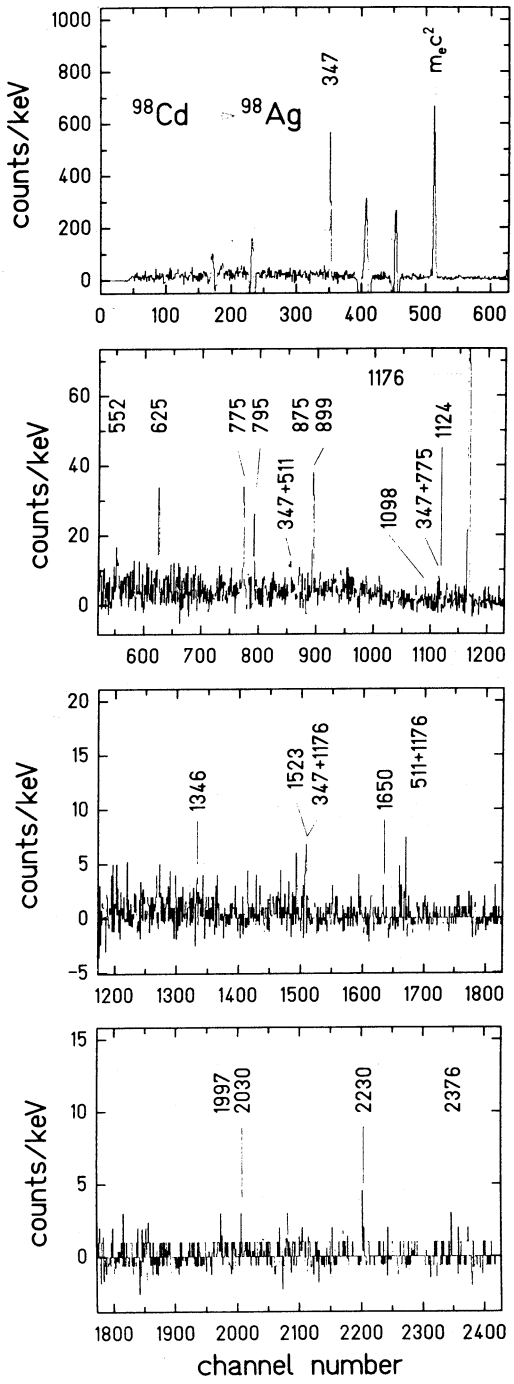

Fig. 2. Sum of eight coincidence γ-ray spectra recorded in the 70% detector, the gates being set on the silver KX-rays and the 61, 107, and 347 keV γ-lines recorded in other detectors (26 h of data acquisition). The structures around 164, 225, 404, and 450 keV originate from scattering of annihilation quanta or intense γ-ray such as the one at 286 keV from ^{75}Br decay (see also caption to Fig. 1).

Table 1. Energies, relative intensities, and coincidence relations for γ-rays following the $^{98}Cd \rightarrow {}^{98}Ag$ decay. One I_γ^{rel} unit corresponds to 0.0008 per ^{98}Cd decay

E_γ (keV)		I_γ^{rel}	Coincident lines
60.55	(10)	450(20)	XAg, 107, 347, 511, 625, 775, 795, 899 1098, 1176, 1523
107.28	(10)	560(14)	XAg, 61, 347, 511, 625, 775, 795, 899 1124, 1176
347.18	(10)	1000	XAg, 61, 107, 511, 552, 625, 775, 874 1176,1346
551.7	(3)	43(6)	107, 347, 625
624.9	(3)	105(15)	XAg, 61, 107, 347, 511, 552, 899
775.6	(4)	60(15)	XAg, 61, 107, 347, 511, 874
794.7	(4)	62(12)	60, 107, 347, 511, 899
874.5	(5)	43(8)	347
898.5	(3)	160(30)	XAg, 61, 107, 511, 625, 795, 1098
1098	(1)	30	
1124	(1)	27(9)	
1176.1	(2)	850(30)	XAg, 61, 107, 347, 511
1346	(1)	20(3)	
1523.0	(5)	44(10)	61, 107
1650	(1)[a]	10	
1996.5	(10)[a]	20	
2030	(1)[a]	20	
2229.5	(10)[a,b]	$\leq$40	
2376	(1)[a]	15	

a) These lines have been observed only in the sum of spectra gated by the 61, 107, 347 keV transitions and the silver KX-rays (see Fig. 2)

b) Not placed in the decay scheme

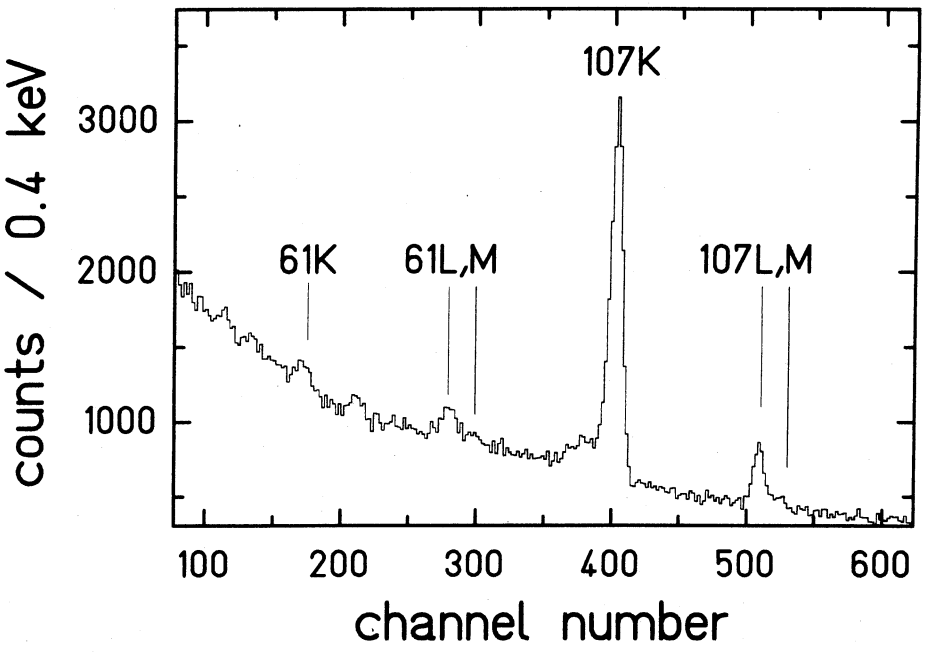

Fig. 3. Electron spectrum measured in the mini-orange spectrometer optimized for recording the K-conversion line of the 107 keV transition (6.8 h of data acquisition). The displayed spectrum covers the energy range between 20 and 123 keV.

Table 2. K-conversion coefficients for low-energy γ-transitions following the $^{98}Cd \rightarrow {}^{98}Ag$ decay

E (keV)	Experiment	Theory [10]		
	this work	E1	E2	M1
60.55	1.80 ± 0.14	0.57	5.45	1.55
107.28	0.82 ± 0.09	0.11	0.87	0.30

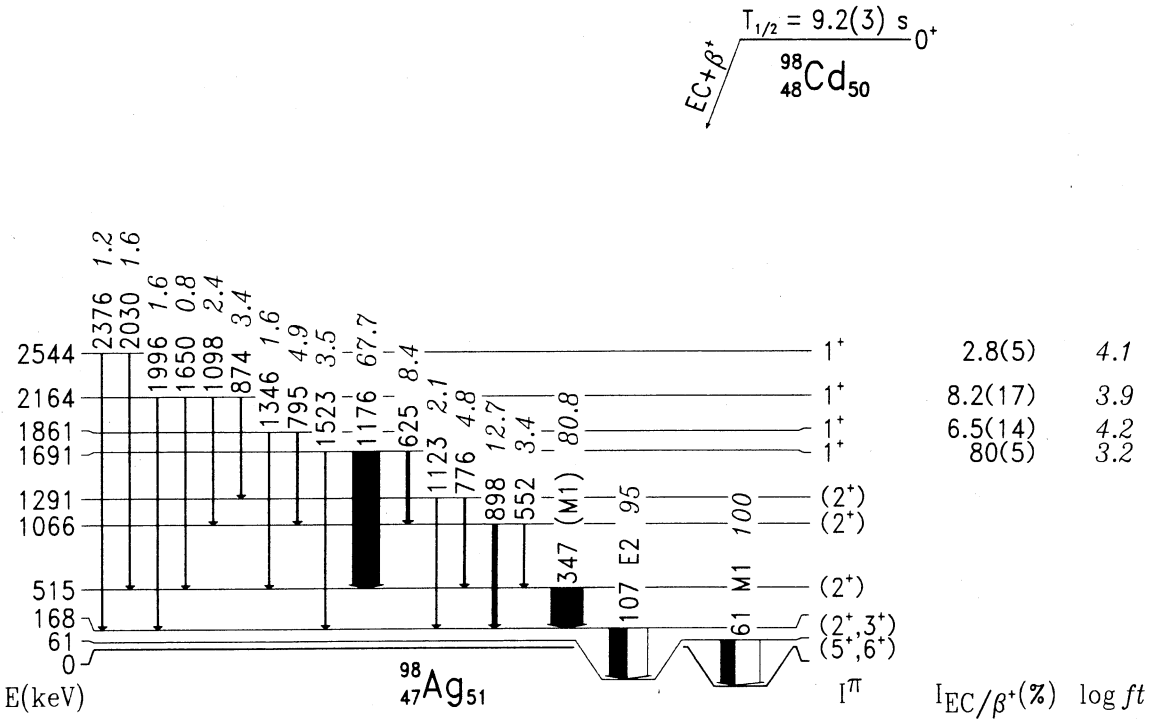

Fig. 4. The decay scheme of ^{98}Cd. The decay energy is based on the extrapolation of data illustrated in Fig. 5. The transitions in ^{98}Ag are marked by their γ-ray energies in keV and total transition intensities per hundred decays (given in italics). The latter quantities were calculated from the intensities given in Table 1, using theoretical [10] total conversion coefficients.

at 1691 keV the assumption of negligible feeding from higher-lying states seems to be safe. In the case of the other three 1^+ levels, this assumption is apparently not quite so well justified. However, a quantitative estimate of the beta-strength observation limit and of the corresponding influence on beta branching ratios and log ft values is not possible, and related effects are therefore neglected in the following discussion of the decay scheme.

The spin and parity assignments to the 1291 keV state and lower-lying levels are not rigorous and can be given only in a tentative way based mainly on systematics. The ground-states of ^{104}Ag, ^{102}Ag, and ^{100}Ag have been identified to be 5^+ [7,11] . If we assume the same assignment for the ground state of ^{98}Ag, the multipole characters of the 61 and 107 keV transitions (and the nonobservation of a 168 keV line) suggest that the 168 keV level is 2^+. The direct feeding of the latter level, presumably by M1 transitions from the 1^+ levels, is compatible with this interpretation. The 107 keV transition has been placed above the 61 keV transition, which is equivalent to proposing the 4^+ level at 61 keV, due to the following consideration: if the first excited state were at 107 keV and had a 3^+ assignment, then one would have observed additional transitions leading to it from levels such as the one at 168 keV. As E2 multipolarity of the transitions to the 168 keV state cannot be ruled out, the spin-parity assignments for the ^{98}Ag ground-state, the 61 keV and the 168 keV level might also be 6^+, 5^+, and 3^+, respectively. This would be consistent with the neigbouring odd-odd isotone ^{96}Rh which has a $I^\pi = 6^+$ ground state [12]. The ^{98}Ag states, situated above the two lowest-lying levels and fed by transitions from the 1^+ states, are presumably 2^+.

4. Discussion

4.1 Shell Model Calculations

Shell model calculations for the N = 50 isotones have been carried out by Gloeckner and Serduke [13] and Blomqvist and Rydström [14] with a ^{88}Sr core, and by Ji and Wildenthal [15] with a ^{78}Ni core. However, no consistent shell model description of $N \geq 50$ nuclei close to ^{100}Sn has been given so far, that would enable a detailed discussion of the decay energies and of the splitting at the GT strength.

In the present work we have used two recent shell model approximations. In the first approach (model A) aimed to describe nuclei with $42 \leq Z \leq 50$ and $50 \leq N \leq 57$, a ^{88}Sr core was assumed, i.e. protons were restricted to the $p_{1/2}$ and $g_{9/2}$ orbit. Neutrons were allowed in the $d_{5/2}$, $g_{7/2}$, $s_{1/2}$, and $d_{3/2}$ orbits. For protons the single-particle energies (SPE) and the two-body matrix elements (TBME) were taken from the sen-

iority conserving set of SPE and TBME given by Gloeckner and Serduke [13]. The neutron SPE are taken from levels in ^{89}Sr, and the proton-neutron TBME, involving the configurations $\pi p_{1/2}(d_{5/2}, g_{7/2}, s_{1/2}, d_{3/2})$ and $\pi g_{9/2}\ \nu d_{5/2}$, are derived from the known multiplets in ^{90}Y. For the $\pi g_{9/2}\ \nu g_{7/2}$ configuration, where no experimental data are available, the Sussex/Yale set of TBME was used [16] . Further details on the SPE and the TBME values used will be given in forthcoming papers on ^{104}Sn [17], $^{100,102,104}Cd$ [18] , and ^{100}Ag [19] .

In a second approach (model B), aimed at N = 50 and 51 nuclei, the $p_{1/2}$ and $p_{3/2}$ proton shells were included using a hypothetical ^{100}Sn core. The $\pi f_{5/2}$ orbit in this mass region is the deepest bound one [15] and can hence be omitted. Single-particle energies and two-body matrix elements were taken from a perturbative treatment of a realistic nucleon-nucleon interaction [20].

4.2 Discussion of Q_{EC} Values

For the accurate determination of the GT strength, the decay energy Q_{EC} for ^{98}Cd ought to be determined with an uncertainty below 100 keV (see Sect. 4.3). In view of the low production rate, this is a difficult task. An attempt to measure the end-point energies for the ^{98}Cd positron spectra with the use of a high-transmission superconducting beta spectrometer failed mainly because the level of molecular contaminants (see Sect. 2) was too high. Therefore one has to rely presently upon extrapolating the Q_{EC} data available for neighbouring even nuclides.

It is well known that decay energies can be approximated, for locally restricted areas of the mass-energy surface, by linear dependences upon N, Z, A etc.. We shall return to the shell-model justification for this linearity in Z or N below. For the cadmium isotopes with mass number 104, 102, and 100, the decay energies, taken from [21], [22], and [7], respectively, show indeed an approximately linear dependence on the mass number (see Fig. 5). For ^{98}Cd, the linear regression gives Q_{EC} = 5.286 MeV. Even better linearity is observed for the Q_{EC} dependence on A for the N = 50 isotones ^{92}Mo, ^{94}Ru, and ^{96}Pd (data from [21]). In this case, the linear Q_{EC} value extrapolation yields 5.369 MeV for ^{98}Cd (and 7.274 MeV for ^{100}Sn).

For further analysis of the ^{98}Cd decay, the average of the extrapolated values, Q_{EC} = 5.33 MeV, is adopted. Its error is assumed to be Δ = 0.14 MeV. This is a sum of contributions from the linear fit Δ_{fit} = 0.06 MeV and from a systematic deviation from linearity, which is estimated to be Δ_{syst} = 0.08 MeV from applying a linear fitting procedure to theoretical Q_{EC} values (see below) for N = 50, Z = 50 parent nuclei. In Fig. 5, the shell-model Q_{EC} values, calculated using shell-model A, are shown. The agreement between experiment and theory, both in the absolute values and in linearity, is

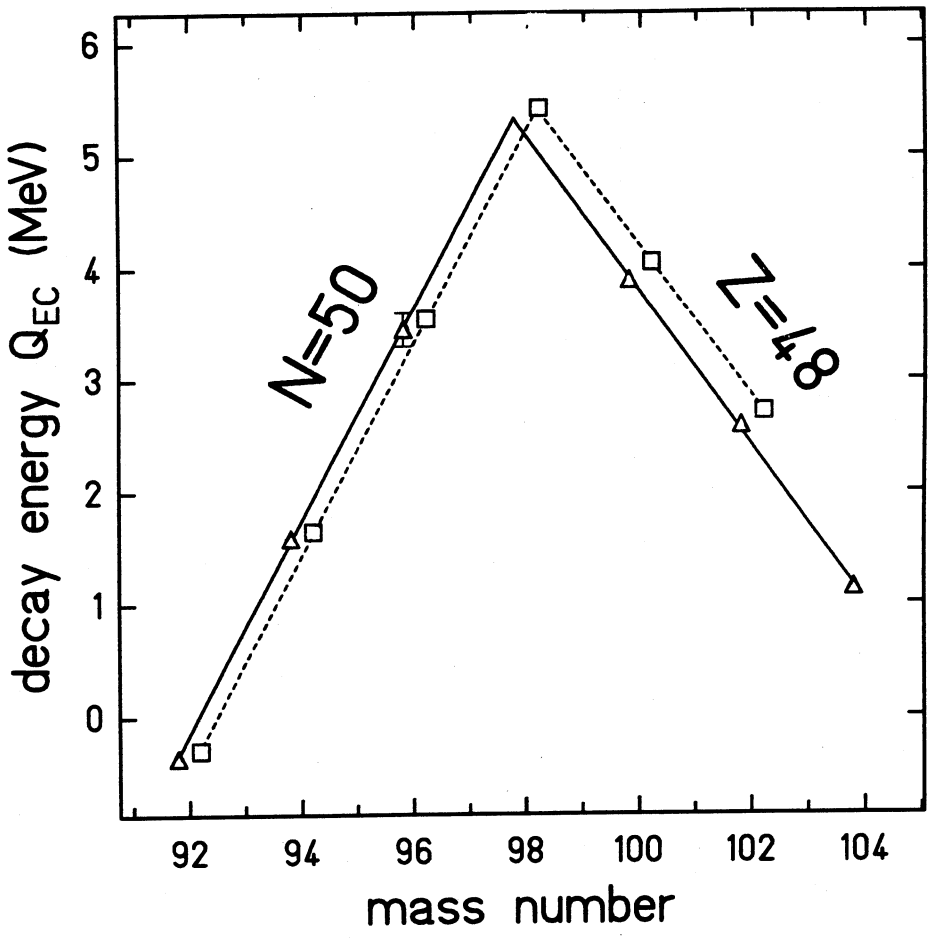

Fig. 5. Q_{EC} values for N = 50 isotones and cadmium isotopes around ^{98}Cd. Data are taken from experiment (triangles) and from shell model A (squares). In the model calculations, the occupation number of the $\nu s_{1/2}$ and $\nu d_{3/2}$ orbits was restricted to 2 for N = 50 nuclei and to 1 for ^{100}Cd. The symbols are drawn slightly aside from the mass-number coordinate in order to avoid overlap. The linear fits that are shown as solid lines are based on measured Q_{EC} values of N = 50 and Z = 48 nuclides, respectively, and are used for the semiempirical determination of the ^{98}Cd Q_{EC} value. The corresponding linear fits of the experimental data and the shell-model results are shown as full-drawn and dashed lines, respectively.

very good, even though a closer inspection reveals small deviations from a linear behaviour, which leads to the above mentioned Δ_{syst} term. The matrix elements used in shell-model A have been chosen to explain many properties of nuclei near ^{100}Sn besides their Q_{EC} values, and we consider this model to be the most appropriate one for estimating the systematic error Δ_{syst}. The adopted value of $Q_{EC} = 5.33 \pm 0.14$ MeV is in good agreement with the prediction of Dobaczewski et al. [23], and with the global mass evaluations of Tachibana et al. [24] , Möller and Nix [24] , and Möller [24], which yield 5.18, 5.40 and 5.34, respectively. However, the other mass formulae in the 1986-1987 mass evaluation [24] predict Q_{EC} values that are several keV larger, and the mass formulae exhibit greater departures from linearity than shell-model A. There remains a doubt about the validity of our procedure for estimating Q_{EC} which can only be resolved by an accurate measurement.

The reason for a linear Q_{EC} dependence can be found in the well known Talmi binding-energy formula in connection with the specific single-particle structure near ^{100}Sn. According to the formula (30.5) in the book by de Shalit and Talmi [25] , n (proton or neutron) valence particles on the orbit j yield a contribution to the total nuclear binding energy of

$$\text{B.E } (j^n) = nC + (n/2)(n-1)a + [n/2]b. \qquad (1)$$

$[n/2]$ stands for the largest integer not exceeding n/2, while C, a, and b are parameters related to the effective interaction between the nucleons. We assume for the following discussion ^{90}Zr (instead of ^{88}Sr [13,14]) as a core, and take into account n = Z-40 protons in the $g_{9/2}$ orbit. In the parent N = 50 isotones, protons are the only particles outside the core. For the relevant odd-odd daughter nuclei, in addition to the protons, also one valence $d_{5/2}$ neutron is present. If we assume that (i) the variation of the binding energy is defined primarily by the number of $g_{9/2}$ protons and (ii) the above formula may be applied to both the parent and daughter nuclei with the same parameters, we get a linear dependence of Q_{EC} on mass number, as observed approximately in the experiment. This is not affected by the residual interaction in the (n-1) daughter, which according to formula (37.18) of ref. [25] is linear in (n-1) in leading order.

Application of these arguments to the cadmium (Z = 48) decay energies is not straightforward. Linearity here may be connected with the dominating role of the neutron $d_{5/2}$ and $g_{7/2}$ orbits which come close in energy approaching Z = 50 and thus act as a single "pseudo" l = 3 orbit in an LS scheme.

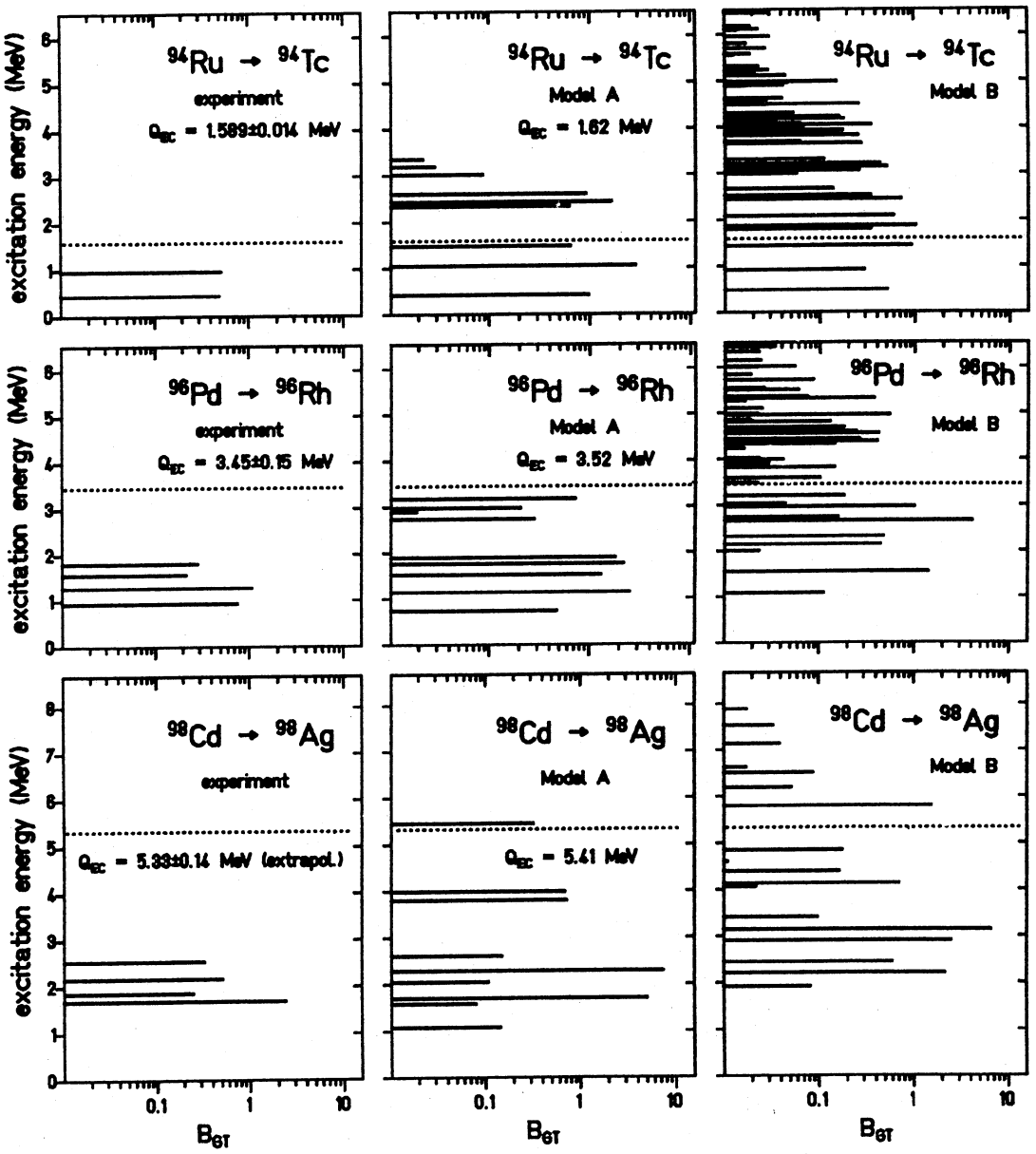

Fig. 6. Strength of the $0^- \rightarrow 1^+$ transitions in the decay of ^{94}Ru, ^{96}Pd, and ^{98}Cd, the N = 50 isotones of ^{100}Sn. The experimental data are from refs. [4, 5] and from this work (see Fig. 4), respectively. For details of the shell-model approaches A and B see text. The dotted lines indicate the upper end of the Q_{EC} windows.

As the first one of several possible quenching mechanisms, we consider pairing, which essentially enters the strength via the proton $\pi g_{9/2}$ and neutron $\nu g_{7/2}$ orbit:

$$B(GT) = (160/9) \times (v_\pi^2) \times (1 - v_\nu^2) \qquad (3)$$

Here, the occupation numbers v^2 for the proton $g_{9/2}$ orbit and the neutron $g_{7/2}$ orbit are taken from the calculations based on the Woods-Saxon average field and on the monopole-pairing residual interaction [24]. For N = 50 isotones, such calculations predict the $\nu g_{7/2}$ orbit to be almost empty, and the and the v_π^2 numbers to be very close to the ones expected from the extreme single-particle shell model, so that there is not much quenching to be expected from pair-correlations.

As an additional quenching mechanism, Towner [2] and more recently Johnstone [34] considered particle-hole residual interactions which lead to a ground-state admixture of the two-particle/two-hole type. For the case of ^{98}Cd , it is mainly the component

$$| (\pi g_{9/2}^{-1} \nu g_{7/2}) 1^+ (\nu g_{9/2}^{-1} \pi g_{7/2})) 1^+, \ 0^+ > \qquad (4)$$

which corresponds to a matrix element of opposite sign relative to the main component, and yields thus a reduction of the GT strength. Depending upon the form of the interaction assumed, one obtains a core-polarisation hindrance $h_{cp} = 1.59...2.19$ [2] and $h_{cp} = 2.08$ [34].

Besides particle-hole, also particle-particle interactions have been considered by several authors [28-31, 35, 36] within the quasiparticle random-phase approximation (QRPA). The effect of the latter is to shift part of the GT strength from low-lying 1^+ states in the daughter nucleus to higher exitation energy.

The shell-model approaches A and B contain at least partly some of the corrections discussed above. Within the applied model space, the main part of the proton-pair correlations is expected to be included. Also the configuration mixing effect, shifting GT strength in the daughter nucleus to higher excited 1^+ states, is contained in the shell model as discussed in Sect. 4.3.2. However, particle-hole core polarization is not included and has thus to be introduced separately.

In Table 3, the experimental quenching of the total GT strength, observed in the beta decays of N = 50 isotones, is compared to the values predicted by the models A and B, and by other approaches described in the literature. The columns 5 and 6 of Table 3 contain the results obtained with the models A and B, taking core-polarization hindrance factors (h_{cp}) [2] and small corrections (h_{vp}) due the neutron pairing [24] into account. This comparison shows that in addition to core-polarization, the splitting of the GT strength, shifting it to higher excitation energy, is essential for the under-

Table 3. GT quenching for the decays of even N = 50 isotones defined with reference to the prediction from the extreme single-particle shell model. The experimental results for ^{94}Ru [4], ^{96}Pd [5] , and ^{98}Cd (this work) are confronted to model pedictions.

Decay of	Experiment	Model A	Model B	Model A including h_{cp}[2] and h_{vp}[23]	Model B including h_{cp}[2] and h_{vp}[23]	Towner [2] without including $h_{high} = 1.6$	Johnstone [34] without including $h_{high} = 1.6$	RPA models			
								[28]	[34]	[29, 32]	[30]
$^{94}_{44}Ru_{50}$	$7.2\ ^{+0.6}_{-0.7}$	1.60	4.11	5.0 - 7.7	11.0 - 17.0	2.9 - 4.4	5.1	7.2	--	5.9	3.1 - 4.1
$^{96}_{46}Pd_{50}$	$4.6\ ^{+1.2}_{-1.7}$	1.12	1.35	2.3 - 3.3	2.8 - 4.0	2.4 - 3.4	3.6	5.9	--	5.6	3.2 - 3.7
$^{98}_{48}Cd_{50}$	$4.1\ ^{+1.0}_{-0.8}$	1.10 *)	1.19 *)	1.8 - 2.5 *)	1.9 - 2.7 *)	2.0 - 2.8	2.7	$25\ ^{+8}_{-2}$	4.2 *)	4.6	--

*) The calculated GT strength was summed over an excitation-energy window from 0 to 3.75 MeV. This interval corresponds roughly to the experimentally accessible one.

standing of the data. Recently such a conclusion has independently been drawn by Johnstone [34], who calculated GT strength distributions for the decays of N = 50 isotones. Johnstone obtained a configuration-mixing part similar to the models A and B, and calculated the core-polarization and pairing-hindrance according to Towner's approach [2] . However, the total hindrance factors given by Towner [2] and Johnstone [34] were additionally corrected by a factor $h_{high} = 1.6$ to account for possible higher-order effects [2, 34]. We did not include the latter correction for the comparison with the experiment, shown in Table 3.

When confronting the measured GT data with theory, one has to take into account that experimental sensitivity limits [37] cannot be given for the three nuclides discussed here. For the case of ^{98}Cd, the ^{98}Ag excitation-energy window for integrating the calculated B(GT) strength has been restricted, in a somewhat arbitrary way, to 3.75 MeV (see footnote in Table 3). No such restrictions have been applied for ^{94}Ru and ^{96}Pd , where the full decay-energy window has been used for determining the quenching factors for the models A and B (see columns 3, 4, 5, and 6 of Table 3).

We conclude on the basis of the data shown in Table 3 that the measured GT strengths seems to be systematically somewhat smaller than the calculated ones. However, at the present level of experimental and theoretical accuracy, there is apparently no need for a correction of higher order effects (i.e. g_A renormalization, see discussion in Sect. 4.3.1): Shell-model approaches, accounting for configuration mixing, pairing effects, and core-polarization, are not far from explaining the entire experimentally observed GT strength and its distribution (see columns 2, 5, and 6 of Table 3 and Fig. 6). The slight disagreements that remain in particular for the ^{98}Cd case (see columns 1, 4, and 5 of Table 3), might well be due the fact, that some of the strength was still missed in the experiment (see Sect. 3.2).

The models using random-phase approximation (RPA) methods (see columns 9, 10, 11, and 12 of Table 3) do not yield a consistent set of results. The approach by Suhonen et al. [28] , overestimates the quenching dramatically for the ^{98}Cd case, probably due to the adjustment of the model parameters to experimental data that have since been updated [38]. The calculations by Kuzmin and Soloviev [29, 32], Borzov et al. [30], and Hirsch et al. [36] seems to be much closer to experiment. However, the calculated GT strength distributions are either not given in the published literature so far [29, 30, 32] or disagree with the expertimental data [36].

As a general trend, emerging also from RPA calculations, the deviations of B(GT) from the B_{ref}(GT) value due to the particle-hole and particle-particle residual interactions decrease systematically when approaching the doubly-closed-shell nuclide ^{100}Sn [37]. The relative importance of higher-order effects (possibly leading to a renormalization of g_A , see Sect. 4.3.1) is expected to increase accordingly. This

emphasizes the importance of measuring decay data for ^{98}Cd compared to those for the lighter N = 50 isotones.

5. Conclusions

Despite of the low production rate of ^{98}Cd, the main features of the decay scheme of this exotic nuclide have been experimentally established. In agreement with shell-model expectations, this decay is dominated by GT transitions. Some information on the splitting and quenching of the GT strength has been obtained, and preliminary tests of the relevant model predictions have been carried out. However, for an improved verification of the theory, further experimental studies are clearly required. Future experiments on the ^{98}Cd decay should focus on (i) a determination of the decay energy with an error below 100 keV and (ii) a search for possible weak beta branching to higher excited states of the ^{98}Ag daughter. Such new data can be compared to the detailed predictions of the shell model A and B for the GT splitting and can thus yield decisive information on the GT quenching. The dominant part of the GT strength of ^{98}Cd is predicted by these models to lie at ^{98}Ag excitation energies below 3.5 MeV. If this pattern is confirmed experimentally at an improved level of accuracy, there may be no space left for additional quenching mechanisms. Such a result would call for a major revision of the present explanation of GT quenching in heavier nuclei. It should be noted, however, that for excitation energies above 3 MeV excitations across the N = 50 major shell will also contribute [39].

Further studies of the EC/β^+ decay of ^{98}Cd and maybe even ^{100}Sn, with their large Q_{EC} values, which according to our semi-empirical estimates are 5.33(14) and 7.3(3) MeV, respectively, thus provide important test cases for solving the puzzle of the GT strength quenching. In this context, it is interesting to note the conclusions drawn by Adelberger et al. [40] from a recent high-resolution study of the ^{37}Ca decay, namely that the claim of GT quenching, based primarily on shell-model analyses of low energy-release beta decay and on (p,n) cross sections, has to be called into question.

References

1. Blomqvist, J.: GSI lecture (1984), unpublished
2. Towner, I.S.: Nucl. Phys. A444, 402 (1985)
3. Kalinowski, V.: Proc. Int. Workshop on Nuclear Structure of the Zirconium Region. J. Ebert et al. (eds), p 397. Berlin, Heidelberg, New York: Springer 1988
4. Graf, P., Münzel, H.: Radiochim. Acta 20, 140 (1987)
5. Rykaczewski, K., Grant, I.S., Kirchner, R., Klepper, O., Koslowski, V.T., Larsson, P.O., Nolte, E., Nyman, G., Roeckl, E., Schardt, D., Spanier, L., Tidemand-Petersson, P., Zganjar, E.F., Zylicz, J.: Z. Phys. A-Atoms and Nuclei 322, 263 (1985)
6. Elmroth, T., Hagberg, E., Hansen, P.G., Hardy, J.C., Jonson, B., Ravn, H.L., Tidemand-Petersson, P.: Nucl. Phys. A304, 493 (1978)
7. Rykaczewski, K., Plochocki, A., Grant, I.S., Gabelmann, H., Barden, R., Schardt, D., Zylicz, J., Nyman, G.: Z. Phys. A-Atomic Nuclei 322, 275 (1989)
8. Ravn, H.L.: Proceedings of a Workshop on the ISOLDE Programme. Allardyce, B.W. et al. (eds), Zinal, Switzerland, June 18-22, 1984
9. Barden, R.: Thesis, Johannes-Gutenberg Universität, Mainz 1988 and GSI-Report, GSI 88-18 (1988)
10. Rösel, F., Fries, H.M., Alder, K., Pauli, H.C.: At. Data Nucl. Data Tables 21, 110, (1978)
11. Lederer, C.M., Shirley, V.S.: Table of Isotopes, 7th Edn, New York: Wiley 1978
12. Piel, W.F., Jr., Fossan, D.B., Ma, R., Paul, E.S., Xu, N., Mc Grory, J.B.: Phys. Rev. 41, 1223 (1990)
13. Gloeckner, D.H., Serduke, F.J.D.: Nucl. Phys. A220, 477 (1974)
14. Blomqvist, J., Rydström, L.: Physica Scripta 31, 31 (1985)
15. X-Ji, Wildenthal, B.H., Phys. Rev. C37, 1256 (1988)
16. Skouras, L.D., Dedes, C.: Phys. Rev. C15, 1873 (1977)
17. Schubart, R., Alber, D., Alfier, R., Bach, C., Fossan, D.B., Grawe, H., Kluge, H., Maier, K.H., Schramm, M., Waring, M., Wood, L.: submitted to Z. Phys. A
18. Alber,D., Berger, A., Bertschat, A.A., Grawe, H., Haas, H., Kluge, H., Kuhnert, A. Mahnke, H.E., Maier, K.H., Schubart, R., Spellmeyer, B., Sun, X., Wood, L.: Nuclear structure study of the neutron-deficient cadmium isotopes $^{100,101,102}Cd$, to be published

19. Alfier, R., Alber, D., Grawe, H., Kluge, H., Maier, K.H., Schubart, R., Fossan, D.B., Piel Jr., W.F.: In beam spectroscopy of neutron-deficient ^{100}Ag, submitted to Z. Phys. A
20. Skouras, L.D., Manakos, P.: Shell-model calculations of β^+ decay of the proton-rich nucleus ^{98}*Cd*, Internal Report IKDA 91/5 (1991)
21. Wapstra, A.H., Audi, G., Hoekstra, R.: At. Data and Nucl. Data Tables 39, 281 (1988)
22. Keller, H., Barden, R., Kirchner, R., Klepper, O., Roeckl, E., Schardt, D., Grant, I.S., Plochocki, A., Rykaczewski, K., Szerypo, J., Zylicz, J.: Z. Phys. A-Hadrons and Nuclei (in print)
23. Dobaczewski, J., Nazarewicz, W., Plochocki, A., Rykaczewski, K., Zylicz, J.: Z. Phys. A-Atomic Nuclei 329, 267 (1988)
24. Haustein, E. (ed.): 1986-1987 Atomic Mass Predictions, At. Data and Nucl. Data Tables 39, 185 (1988)
25. de Shalit, A., Talmi, I.: Nuclear Shell Theory. New York, London: Academic Press 1963
26. Bohr, A., Mottelson, B.R.: Nuclear Structure. Vol.1, p. 349. New York: Benjamin 1969
27. Häusser, O.: Proc. Fifth Int. Conf. on Nuclei far from Stability, AIP Conference Proceedings 164. Towner, I.S. (ed.), p. 604. New York: American Institute of Physics 1988
28. Suhonen, J., Taigel, T., Faessler, A.: Nucl. Phys. A 486, 118 (1988)
29. Kuzmin, V.A., Soloviev, V.G.: Modern Phys. Lett. A3, 1533 (1988)
30. Borzov, I.N., Trykov, E.L., Fayans, S.A.: Sov. Journal of Physics,. in print
31. Suhonen, J.: Phys. Lett. 255B, 159 (1991)
32. Kuzmin, V.A., Soloviev, V.G.: Czechoslovak Journal of Physics, in print
33. Barden, R., Kirchner, R., Klepper, O., Plochocki, A., Rathke, G.-E., Roeckl, E., Rykaczewski, K., Schardt, D., Zylicz, J.: Z. Phys. A-Atomic Nuclei 329, 319 (1988)
34. Johnstone, I. P.: "Gamow-Teller Decay of N = 50 Nuclei", submitted to Phys. Rev. C
35. Cha, D.: Phys. Rev. C27, 2269 (1983)
36. Hirsch, M., Staudt, A., Muto, K., Klapdor-Kleingrothaus, H.V.: Proc. 6th Workshop on Nuclear Astrophysics, Ringberg, Febr. 1991, in print, Internal Report MPIH-V11-1991, and M. Hirsch, private communication (1991)
37. Klepper, O., Rykaczewski, K.: GSI Preprint GSI-90-63, contribution to the Predeal Int. Summer School on Recent Advances in Nuclear Structure, Predeal, Romania, August 28-September 8, 1990

38. Rykaczewski, K., Barden, R., Gabelmann, H., Grant, I.S., Hill, P., Keller, H., Kirchner, R., Klepper, O., Kolasinski, A., Pfützner, M., Plochocki, A., Ravn, H., Roeckl, E., Schardt, D., Szerypo, J., Thorsteinsen, T., Zylicz, J.: Proc. XXI Int. Summer School on Nuclear Physics, Mikolajki, Aug. 26 - Sept. 5, 1990
39. Alber, D. et al.: Z. Phys. A-Atoms and Nuclei 335, 265 (1990)
40. Adelberger, E.G. et al., "Is the weak axial current renormalized in nuclei?", to be published